

## Process Flow for Fabrication and Characterization of AlGaN/GaN High Electron Mobility Transistors

In this chapter, the process flow, which is used for device fabrication for AlGaN/GaN HEMT and its electrical characterization, will be discussed. Starting from the epitaxial growth of AlGaN/GaN HEMT layers on Si (111) substrate to the characterization of the AlGaN/GaN HEMT wafer and the fabrication of the device by optical lithography will be explained. The characterization of AlGaN/GaN HEMT wafer includes X-ray diffraction, atomic force microscopy (AFM), and transmission electron microscopy (TEM) analysis. Furthermore, the device characterization process will be discussed. These AlGaN/GaN HEMT structures were utilized in the heavy metal ion sensing applications, which will be discussed in upcoming chapters.

### 4.1 EPITAXIAL GROWTH OF AlGaN/GaN HEMT ON SI (111) SUBSTRATE

As described in chapter 3, this work collaborates with IIT Jodhpur and the Institute of Materials Research and Engineering (IMRE), A\*STAR Singapore. In this collaboration, the growth of AlGaN/GaN heterostructures was performed by the IMRE scientists, and the device fabrication and their development as heavy metal ion sensors were carried out by the author at IIT Jodhpur. The epitaxial growth of the  $\text{Al}_x\text{Ga}_{1-x}\text{N}/\text{GaN}$  HEMT was carried out on 2-inch diameter Si (111) substrates by the AIXTRON CCS 19×2-inch MOCVD system refurbished at IMRE. Figure 4.1 shows the epitaxial structure of the grown AlGaN/GaN HEMT. Here, the 2-inch, p-type Si wafer with (111) orientation is utilized. The epitaxial growth of the layers is initiated by an in-situ oxide cleaning of the wafer surface through the flow of hydrogen in the MOCVD reactor. Furthermore, the pretreatment of trimethyl-aluminum was also performed for a short period. Moreover, a 120 nm thick AlN nucleation layer was overgrown on Si (111) substrate. The growth process was further carried out by the deposition of step-graded intermediated layers of  $\text{Al}_x\text{Ga}_{1-x}\text{N}$  of 700 nm thickness. For the nitride layers, the growth parameters varied from the reactor to reactor; however, the growth temperature of the AlN nucleation layer, Al content in intermediate layers, and gas flow mechanisms are kept constant for the epitaxial growth of the GaN channel region. In general, the typical surface temperature for the epitaxial growth of GaN is kept around 1040°C, and trimethylgallium is utilized as a precursor of Ga. In this process, an uninterrupted epi layer growth of 900 nm GaN is executed. During this, an intentional low pressure tuning at the AlGaN interlayer and GaN interface incorporates a background carbon doping in the GaN buffer layer; thus, this layer is also known as unintentionally doped (UID) GaN layer. Furthermore, an undoped GaN layer of 150 nm thickness is grown over this UID GaN layer. This layer is called a GaN channel layer. In the top layer of this heterostructure, the HEMT stack has a thin AlN spacer layer of 1 nm, 22 nm  $\text{Al}_{0.23}\text{Ga}_{0.77}\text{N}$  barrier layer, and an undoped GaN cap layer of 2 nm thickness. The complete epitaxial growth of this HEMT structure has 1.8  $\mu\text{m}$ .

The AlGaN/GaN HEMT structure utilized for the simulation analysis is also grown in a similar way by MOCVD at IMRE A\*STAR Singapore and is shown schematically in Figure 2.2 (d). Here, the AlGaN/GaN HEMT structure was overgrown on a 200 mm Si (111) wafer. A low-temperature AlN nucleation layer of the thickness 25 nm followed by 373 nm high-temperature

AlN nucleation layer at 75 torr has been grown on a silicon substrate. Other intermediate AlGaN layers are tuned accordingly to make crack free GaN layer. In this process, three step-graded AlGaN layers are grown on the nucleation layer with tuned mole fraction  $\text{Al}_{0.60}\text{Ga}_{0.40}\text{N}$ ,  $\text{Al}_{0.40}\text{Ga}_{0.60}\text{N}$ , and  $\text{Al}_{0.20}\text{Ga}_{0.80}\text{N}$ . Furthermore, trimethylgallium is used as the precursor of Ga for GaN growth. The  $2.4\ \mu\text{m}$  GaN layer is uninterruptedly grown above these AlGaN interlayers. As explained above, here also an intentional low-pressure tuning at the heterointerface of  $\text{Al}_{0.20}\text{Ga}_{0.80}\text{N}$  causes background carbon doping. In the top layers, the structure consists of a 1 nm thin AlN spacer layer, an AlGaN barrier layer with an Al mole fraction of 23%, and an undoped cap layer of GaN about 22 nm and 5 nm, respectively. The total stack thickness of the III-N layers is approximately  $4.4\ \mu\text{m}$  [Bhat *et al.*, 2014]. Each epitaxial layer in the AlGaN/GaN HEMT has its importance and was described in chapter 1 in detail. After the epitaxial growth of AlGaN/GaN HEMTs, the developed wafers and growth parameters were provided by the IMRE scientists to the author as per the collaboration.

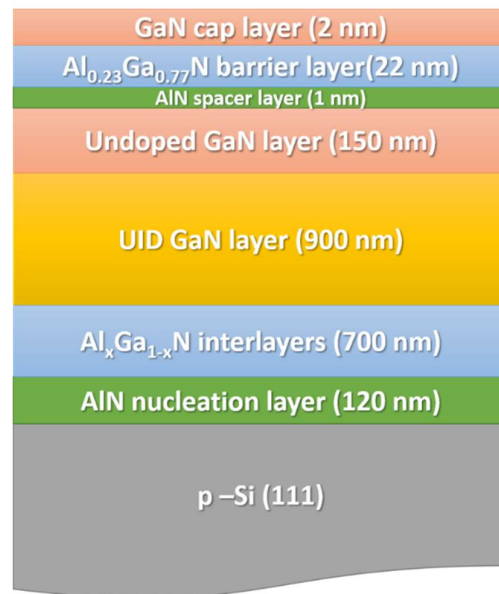


**Figure 4.1:** Epitaxial structure of AlGaN/GaN HEMT grown by MOCVD.

## 4.2 STRUCTURAL ANALYSIS OF AlGaN/GaN HEMT WAFER

The structural analysis of the AlGaN/GaN HEMT wafer was performed by utilizing different morphological processes such as AFM and TEM processes, and the crystalline behavior of the epilayers is obtained by high-resolution X-ray diffraction (HRXRD) process. Each process gives a comprehensive view of the epitaxial growth of the HEMT layers, which significantly impacts the device performance.

### 4.2.1 TEM Analysis

The TEM process is a very efficient tool to observe the structural morphology of the epitaxial growth of the AlGaN/GaN HEMT structure. The operation of the TEM process was explained in chapter 3. The optimized thicknesses of the layers are determined by the cross-sectional transmission electron microscopy (TEM) and are shown in Figure 4.2. This structure was utilized for the experimental analysis and correlation with the simulation studies, as discussed in chapter 2. The top layers of the epitaxial structure demonstrate the GaN/AlGaN/AlN/GaN layers, which is shown in the enlarged view of the structure, whereas the bottom layers, including the AlN nucleation layer, three step-graded AlGaN layers, and GaN buffer layer is also shown in Figure 4.2. The cross-sectional TEM image showed the growth of sharp interfaces of epitaxial layers where the thickness of each layer can be easily measured. Here

the total stack thickness of 4.4  $\mu\text{m}$  has been observed. This structure of AlGa<sub>N</sub>/Ga<sub>N</sub> HEMT was utilized for the simulation studies under the experimental analysis. The schematic view of this structure is depicted in Figure 2.2 (d).

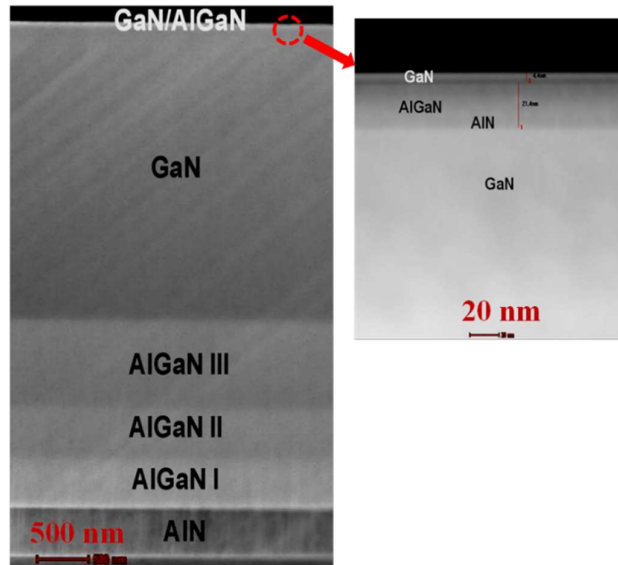


**Figure 4.2:** Cross-sectional TEM of the AlGa<sub>N</sub>/Ga<sub>N</sub> HEMT structure

#### 4.2.2 HRXRD Analysis

High-resolution X-ray diffraction (HRXRD) pattern of the as-grown AlGa<sub>N</sub>/Ga<sub>N</sub> HEMT structures grown over 200 mm Si (111) wafer are shown in Figure 4.3. It was performed to analyze the crystalline behavior of the grown epilayers [Bhat *et al.*, 2014; Longobardi *et al.*, 2014; Tham *et al.*, 2016; Tham *et al.*, 2015]. In this, the XRD pattern was analyzed at three different locations of the HEMT wafer, i.e., center, middle, and edge. The observed diffraction peaks from the XRD scan indicate the presence of AlN nucleation layers, the step-graded AlGa<sub>N</sub> I, II, and III layers, and the Ga<sub>N</sub> layer. Here the dominant peak is for Ga<sub>N</sub> (0002). It has been observed from Figure 4.3 that there are no substantial shifts in the diffraction peaks of these epilayers in the spectrum, indicates no change of strain-composition profile of the structure [Bhat *et al.*, 2014]. The full width at half maximum (FWHM) values calculated from the Ga<sub>N</sub> (0002) peaks are 407, 404, 421 for the center, middle, and the edge of the wafer, demonstrates an adequate uniformity in the crystalline quality of the wafer [Bhat *et al.*, 2014].

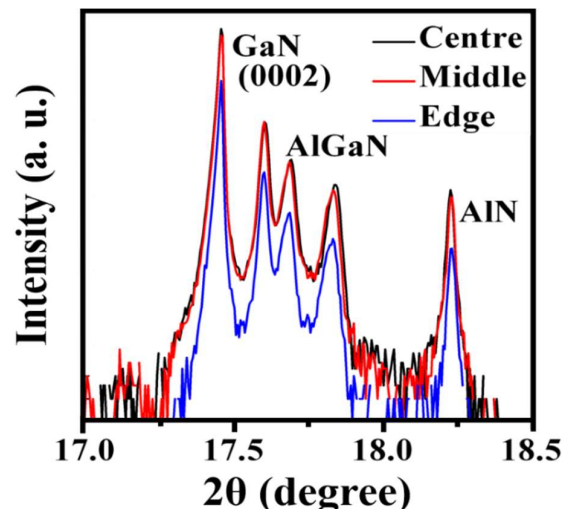


**Figure 4.3:** HRXRD of the epilayers of the AlGa<sub>N</sub>/Ga<sub>N</sub> HEMT structure

### 4.2.3 Surface Analysis of AlGaIn/GaN HEMT Wafer

The AFM process also performed the surface morphological analysis of the prepared AlGaIn/GaN HEMT wafer. By performing AFM analysis on different places of the HEMT wafer similar to the XRD process, the extremely smooth surface is observed throughout the wafer without any significant changes in root mean square (RMS) roughness. The observed AFM morphology in  $5\ \mu\text{m} \times 5\ \mu\text{m}$  over the distinct places is shown in Figure 4.4. The surface steps indicate smooth surface morphology. The observed RMS roughness from AFM analysis across the HEMT wafer is in the range of 0.2–0.3 nm, demonstrates superior surface morphology [Bhat *et al.*, 2014].

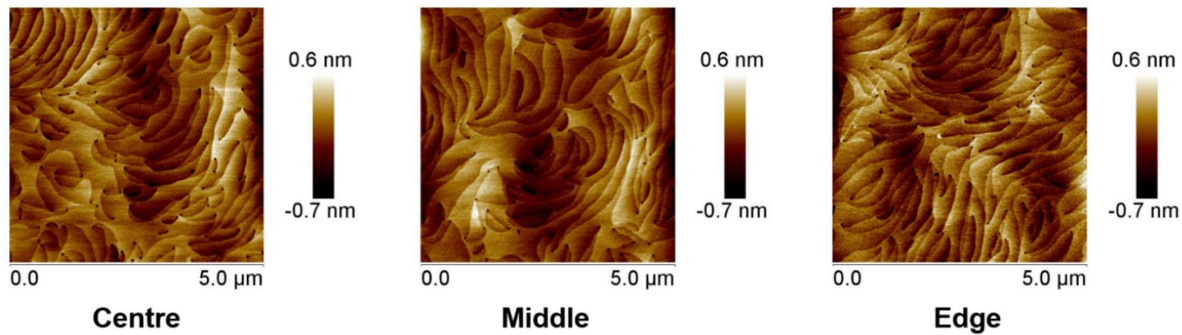


Figure 4.4: AFM morphology of the surface of the AlGaIn/GaN HEMT wafer

### 4.3 FABRICATION OF AlGaIn/GaN HEMT FOR ION SENSING APPLICATION

After the epitaxial growth of the AlGaIn/GaN HEMT structure, the fabrication of AlGaIn/GaN HEMT was performed. Before starting the fabrication process, the sample cleaning is an essential process which can enhance the device quality and fabrication yields. The organic and inorganic dust particles on the surface of the sample not only cause improper and undesirable results but can cause device failure also. Thus, in other words, it can be said that the sample cleaning is the first step towards device fabrication. In order to perform the sample cleaning of AlGaIn/GaN HEMT samples, they were ultrasonicated in acetone for 10 minutes; in this process, the organic impurities from the wafer as well as other dust particles were removed. After this process, they were heated at  $100^\circ\text{C}$  in isopropyl alcohol (IPA) for 10 minutes in order to remove any strain forms at the surface due to acetone application; after that, the sample is washed through deionized water. Moreover, the sample is dipped into warm hydrochloric acid (HCl) to remove the inorganic impurities from the sample. Subsequently, the samples were dipped in deionized (DI) water and dried using a nitrogen gun. Now, the sample is ready for further processing.

The process steps utilized for the fabrication of AlGaIn/GaN HEMT for heavy metal ion sensing applications are shown in Figure 4.5. It includes the source and the drain contact formation, passivation of these contacts by  $\text{Si}_3\text{N}_4$ , the formation of gate contact, and extension of the source and the drain contacts. The description of each step will be described along with the process steps and utilized parameters in the upcoming sections.

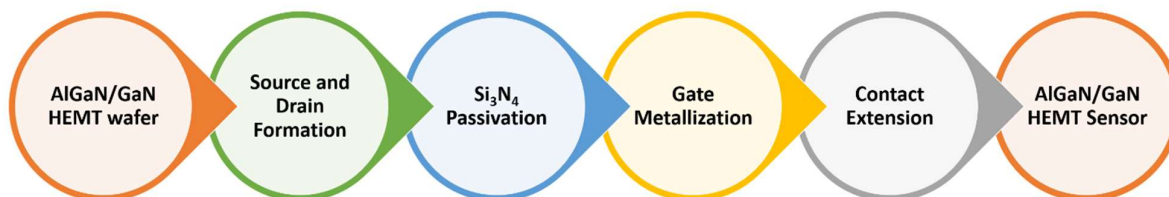
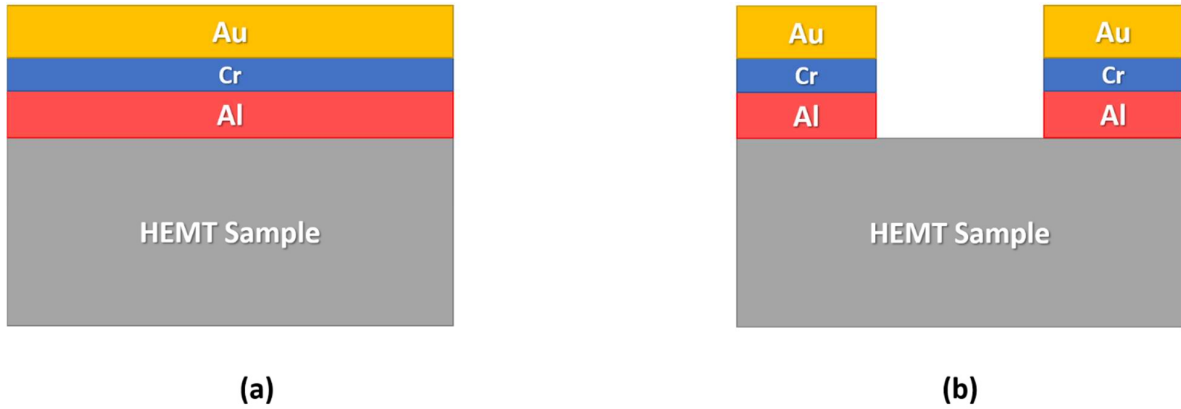


Figure 4.5: Process flow for AlGaIn/GaN HEMT sensor fabrication.

### 4.3.1 Formation of Source and Drain Contacts

In the AlGaN/GaN HEMT device, the source and drain contact is made ohmic to make an electrical connection of the 2DEG channel to the external environment. These contacts should have low resistance as the higher contact resistance significantly affects the performance of AlGaN/GaN HEMT. In order to make these contacts less resistive, the metal contact should possess a low work-function that provides an easy path to allow the electrons through the metal-semiconductor interface. Here, a stack of three metals has been utilized, which are Aluminum (Al), Chromium (Cr), and Gold (Au). These metals provide the ohmic contacts and hence utilized for the formation of source and drain contacts.

The deposition of Al, Cr, and Au was performed by the thermal evaporation process. In this process, the chunks of these metals have been kept in the three-boat thermal evaporation system. The explanation of this thermal evaporation system has been given in chapter 3. In order to get the high mean free path as well as high-quality deposition of the metals, the high vacuum has been created in the system of the order of  $10^{-6}$  mbar. Once the vacuum is reached, the Al evaporation process is started by the continuous increment of current. In this process, two points came, which are given as melting and evaporation point. The current at which the Al or other metal starts melting is called melting current, and the current at which the Al or other metal start evaporating is called evaporating current. The melting and evaporation current for each metal is different. Once the Al or other metal starts evaporation, the thickness and rate of deposition are observed by crystal monitor. Here, the Al was deposited around 150 nm. Once it is deposited, one can reduce the current and of the shutter of the Al boat in order to stop the Al deposition. Similarly, the Cr and Au deposition was also carried out. The Cr and Au were deposited around 30 nm and 200 nm, respectively. Figure 4.6 (a) illustrates the schematic representation of the deposited Al/Cr/Au layers on the AlGaN/GaN HEMT sample.



**Figure 4.6:** Schematic illustration of (a) deposition of Al/Cr/Au metals over HEMT sample by thermal evaporation (b) patterning of the metals for source and drain contact formation using photolithography

Once these metals have been deposited on the AlGaN/GaN HEMT structure, the optical lithography process has been carried out to pattern the source and drain contacts. The explanation of the step by step process has been already given in chapter 3. In order to process those steps for the patterning, the S1813 photoresist was employed on the samples, and the spin coating process was performed. In the spin coating process, the resist was coated at 5000 rpm for 30 s to form a photoresist layer on the surface of the sample. Subsequently, these samples were soft baked at  $100^{\circ}\text{C}$  for 60 s. Then, the samples were aligned under photomask at the respective pattern and get UV exposure. Further, the samples were developed in the CD-26 developer solution for 55 s and dipped into the deionized (DI) water to stop further development reactions. After the development of the photoresist, the post-exposure bake process has been taken place in which samples were get heated on the hot plate at  $110^{\circ}\text{C}$  for 180 s. Furthermore, the etching process has been carried out to remove the metals from the exposed region of the samples. In this work, the

wet chemical etching process has been performed. Since the deposited metal state was Al/Cr/Au, therefore, the Au was etched first.

The Au etching was performed by KI (potassium iodide) solution. After removal of Au from the exposed region of the surface, the chromium etching is performed. For the chromium etching, the chromium etchant has been made by using perchloric acid (86  $\mu$ l), ammonium cerium nitrate (329 mg), and DI water (20 ml). This etchant etches the chromium with 80 Å/min etch rate. After the removal of chromium, the aluminum was etched from the surface of the sample by the orthophosphoric acid, nitric acid, and DI water in the ratio of 16:3:1. By the removal of aluminum from the surface of the sample, the etching process is completed. In the last step, acetone was applied to the sample to remove the photoresist, and the device structure after the photography process looks similar, as shown schematically in Figure 4.6 (b).

After the photolithography, the annealing process was performed to diffuse these contacts in order to make the electrical contact from the 2DEG channel. In this process, the sample was heated at 850°C for 60 s under a nitrogen environment. These samples were then removed and ready for the next process. This complete process forms the source and drains contacts on the AlGaN/GaN HEMT sample.

#### 4.3.2 Si<sub>3</sub>N<sub>4</sub> Passivation

The passivation process of the AlGaN/GaN HEMT is very crucial while it is utilized in heavy metal ion sensing applications. This passivation layer removes the interaction possibilities between the electrical contacts such as source and drain and the ionic solution. This layer also saves the device from a short circuit. This layer should be chemically and mechanically stable in both acidic and basic mediums. Thus, Si<sub>3</sub>N<sub>4</sub> is an ideal candidate for passivation.

The passivation process has been carried out by the deposition of Si<sub>3</sub>N<sub>4</sub> using RF sputtering. A detailed description of RF sputtering has been given in chapter 3. In this process, the Si<sub>3</sub>N<sub>4</sub> target is mounted in the sputtering system, and the process chamber is vacuumed. When the high vacuum in the process chamber is achieved by utilizing a turbomolecular pump, the gate valve towards the turbomolecular pump is partially closed. Subsequently, the carrier gas (Ar) and reactive gas (N<sub>2</sub>) with an optimized controlled flow rate of 45 SCCM and 10 SCCM, respectively, have been inserted into the process chamber through MFC. Once the chamber pressure has reached the optimum value, the RF power is turned on, which ionizes the Ar gas, and plasma is formed. The N<sub>2</sub> gas not only participates in the reaction but also catalyzes the process. Hence the deposition rate increases. In this process, the Si<sub>3</sub>N<sub>4</sub> deposition was performed with a 100 W RF power supply, and the deposition process continues until 2 hrs.; Hence a 250 nm thick Si<sub>3</sub>N<sub>4</sub> layer was deposited over the sample.

The passivation layer is further patterned to make a window in the gate region of the AlGaN/GaN HEMT. This patterning of the passivation layer was carried out by the optical lithography process. The photolithography process steps are similarly followed as the source and drain formation process, except the photomask pattern was aligned on the source and drain contacts by matching the alignment marks available at the photomask and the sample. In the etching process, the Si<sub>3</sub>N<sub>4</sub> was etched out by the diluted HF solution having the HF: H<sub>2</sub>O in the ratio of 1:10. This is the rapid etchant for Si<sub>3</sub>N<sub>4</sub>. Further, the photoresist was removed by the application of acetone on the sample. The schematic demonstration in Figure 4.7 (a) indicates the Si<sub>3</sub>N<sub>4</sub> encapsulation of the source and contacts after the deposition and patterning process.

#### 4.3.3 Gate Metallization and Patterning

The gate metallization is the third level of the HEMT device fabrication process step. The gate contact is crucial as it modulates the carrier concentration in 2DEG; thus, the gate contact should be of Schottky contact so that the gate leakage would be minimum. In order to make the gate an effective Schottky contact, the choice of metals is very crucial and should have good

adhesion to the GaN surface, chemically and mechanically stable, and should have a high work function to reduce the leakage current. To fulfill this requirement for the gate terminal, the combination of Ni and Au as a metal stack is most suitable. The Ni/Au provides good Schottky contact to the GaN. The Ni provides the best adhesion to the GaN surface. It also has a work function of 5.15 eV, which is closer to gold. The Au layer is utilized to prevent the oxidation of the Ni layer and improve the conductivity of the gate. In order to perform the Ni/Au metallization, the thermal evaporation system is utilized. By performing the thermal evaporation process, the 10 nm and 50 nm thin layers of Ni and Au were deposited.

The patterning of the gate is the most challenging task in the AlGaIn/GaN HEMT fabrication process as a very thin contact is patterned. Thus, the patterning of the gate terminal is accomplished by performing the careful alignment process and utilizing similar photolithographic steps, as explained earlier. Subsequently, in the etching process, the Ni was etched by dilute HNO<sub>3</sub> solution, and Au was KI solution. The schematic of the gate patterning is shown in Figure 4.7 (b), and correspondingly the microscopic image of the patterned gate over AlGaIn/GaN HEMT is shown in Figure 4.7 (c). Furthermore, the optical microscopic image of the plan view of the complete fabricated device is shown in Figure 4.7 (d). Here, the gate length ( $L_G$ ), the gate to drain ( $L_{GD}$ ), the gate to source spacing ( $L_{GS}$ ), and drain to source spacing ( $L_{DS}$ ) of the device are 50  $\mu\text{m}$ , 25  $\mu\text{m}$ , 25  $\mu\text{m}$ , and 100  $\mu\text{m}$  respectively. The extended contact pads were further utilized for the contact extension, which will be helpful in sensing the application of the device.

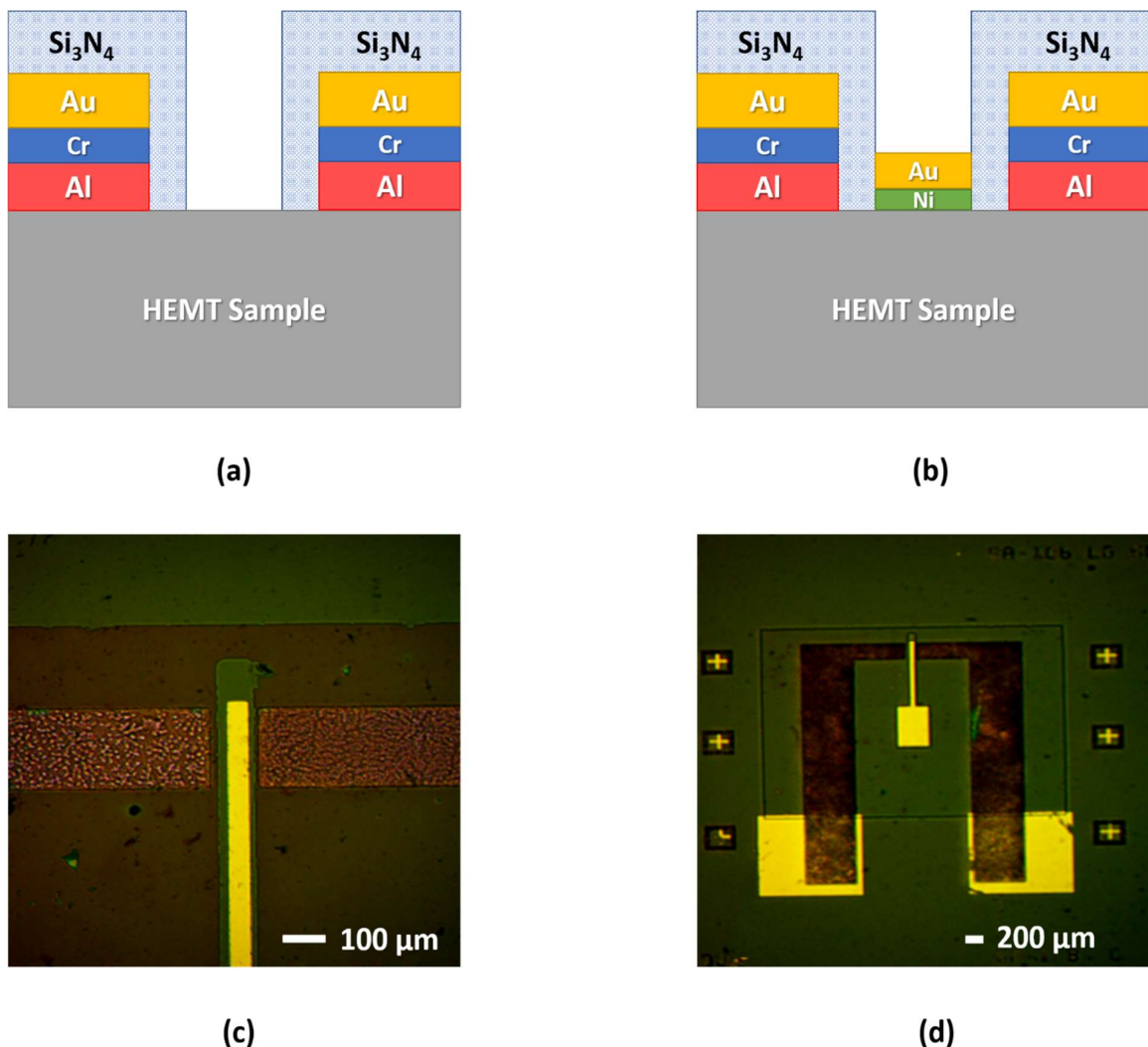


**Figure 4.7:** (a) Schematic illustration of Si<sub>3</sub>N<sub>4</sub> patterning on AlGaIn/GaN HEMT (b) Gate patterning on AlGaIn/GaN HEMT (c), (d) Images of fabricated devices by following the fabrication process steps

#### 4.3.4 Contact Extension process

In order to utilize the AlGaN/GaN HEMT for heavy metal ion sensing applications, the source and drain contacts of the device were extended. In this process, the developed sensor was pasted on the strip of completely etched printed circuit board; then, contact extension was done with the help of silver (Ag) paste and very thin Cu wire. The thin Cu wire is attached with source and drain terminals through Ag paste and insulated with water-resistant material. This device was then utilized for heavy metal ion sensing application by only exposing the gate region in the water or ionic solution while all other portion of the sensor is completely insulated. The device mounting on the PCB and its contact extended view is shown in Figure 4.8.

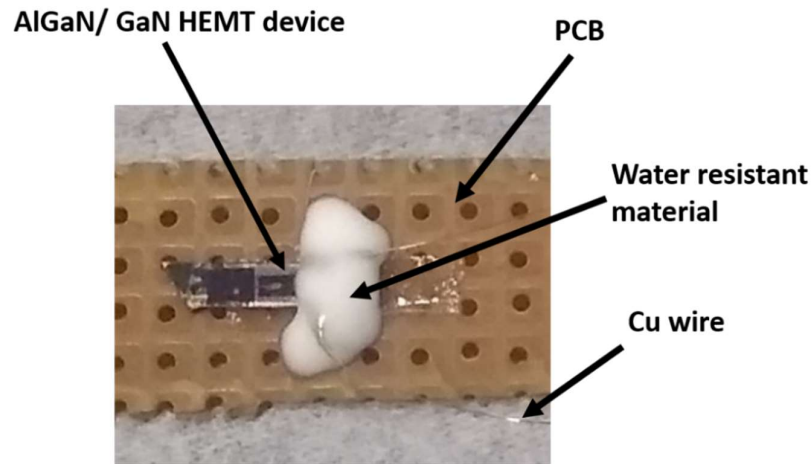


Figure 4.8: Device mounting on PCB and contact extension for Sensing application

### 4.4 ELECTRICAL CHARACTERIZATION OF AlGaN/GaN HEMT

#### 4.4.1 Transmission Line Model (TLM) Process

Transmission Line Model (TLM) is the widely used technique to analyze the electrical properties and the quality of the Ohmic contacts of the AlGaN/GaN HEMT. This process was given by two scientists Reeves and Harrison [Reeves and Harrison, 1982]. In this method, a series of rectangular metal contacts, showing ohmic behavior, are fabricated with continuously increasing spacing. The schematic of the TLM process is shown in Figure 4.9 in which the contact pads are separated by the spacing  $L$ . Here,  $W$  is the width of the contact pads.

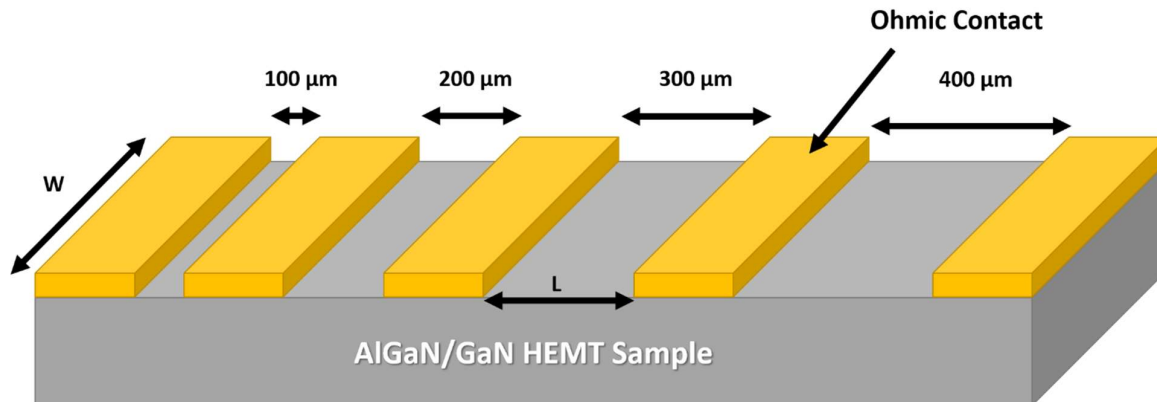


Figure 4.9: Schematic of TLM structure

In this work, the TLM process was carried out by observing I-V characteristics between two contact pads and calculating the total measured resistance  $R_T$ . Subsequently, a graph between



$R_T$  and  $L$  is plotted, and linear fitting to the data points is carried out, as shown in Figure 4.10. Furthermore, the  $R_T$  can also be given as [Taking, 2012]:

$$R_T = 2R_C + R_{Sh} \frac{L}{W} \quad (4.1)$$

where  $R_{Sh}$  is sheet resistance of the semiconductor (here AlGaIn/GaN HEMT) given in  $\Omega/\square$ , and  $R_C$  is contact resistance in  $\Omega\text{-mm}$ . The slope of the linear calibration curve in Figure 4.10 gives the value of  $R_{Sh}/W$ , and its intercept at the y-axis gives the value of  $2R_C$ .

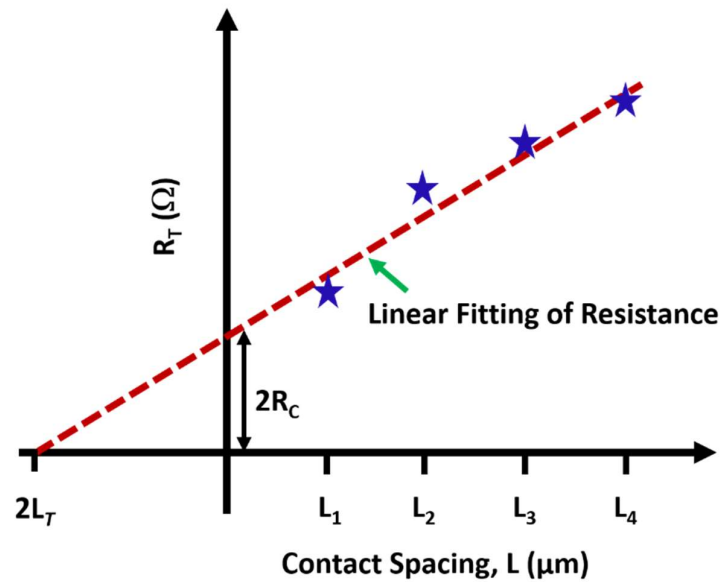


**Figure 4.10:** Explanatory graph for TLM calculation

As per the discussion on the TLM process, the electrical characterization was carried out for the AlGaIn/GaN HEMT structure. Here the I-V characterization between two successive contacts has been performed using Keithley-4200 SCS. The fabricated structure for the TLM process on AlGaIn/GaN HEMT sample is shown in Figure 4.11. These contacts were fabricated using the same approach utilized for source and drain contact formation in the AlGaIn/GaN HEMT device. These contacts possess the same metal stack, i.e., Al/Cr/Au, with the same thickness specifications 150/30/200 nm. These contact pads were separated with the spacing of 100, 200, 300, and 400  $\mu\text{m}$ . The width,  $W$ , and length,  $d$  of these contacts are 1000  $\mu\text{m}$  and 500  $\mu\text{m}$ , respectively.

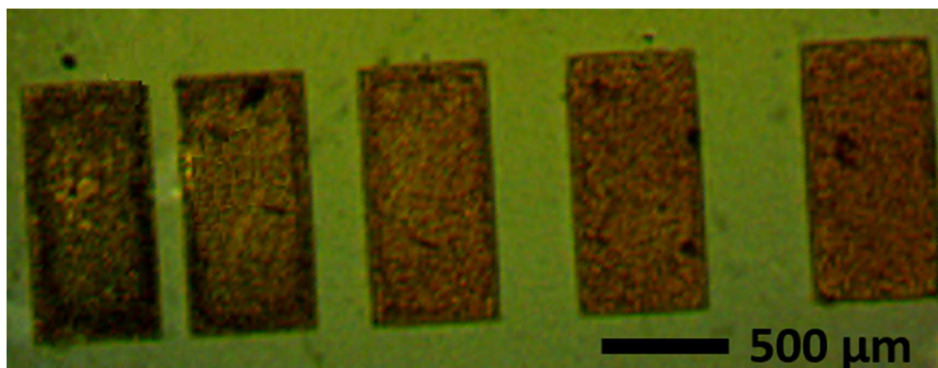


**Figure 4.11:** Optical microscopic image of the fabricated TLM structure

The I-V characteristics of the TLM structure at different contact spacing are shown in Figure 4.12 (a). It has been observed that the characteristics are ohmic. It indicates that the Al/Cr/Au contacts show ohmic behavior with AlGaIn/GaN HEMT structure. Here, the current  $I_{12}$  describes the current observed between contact pad 1 and contact pad 2, having the spacing  $100 \mu\text{m}$ . Similarly,  $I_{23}$  indicates current between contact pad 2 and pad 4, having a distance of  $200 \mu\text{m}$  and so on. Subsequently, the average resistance between each successive contact pad is calculated and plotted as a function of spacing  $L$ , as depicted in Figure 4.12 (b). Furthermore, the linear calibration process was carried out to calculate the sheet resistance  $R_{sh}$  and contact resistance  $R_C$ . The value of  $R_C$  is independent of the  $d$ , whereas it depends only on the width  $W$ , i.e., perpendicular to the flow of current. Thus, the normalized contact resistance was calculated by the multiplication of  $W$  in the value of  $R_C$ , and hence the value of  $R_C$  is given in terms of  $\Omega\text{-mm}$  [Taking, 2012]. By performing the calculation as described above, the value of  $R_C$  is determined as  $34.57 \Omega\text{-mm}$ , and the  $R_{sh}$  is calculated as  $230.88 \Omega/\square$ . Here, the correlation coefficient ( $R^2$ ) was observed as  $0.98971$ .

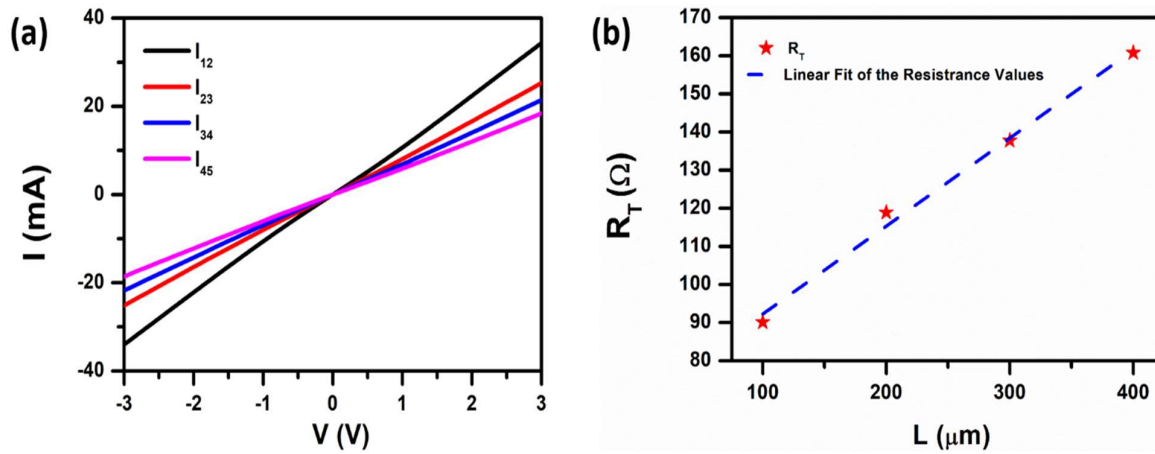


**Figure 4.12:** (a) I-V characteristics at different contact spacing and (b) Observed resistance of the AlGaIn/GaN HEMT TLM structure with respect to the spacing of two successive contacts

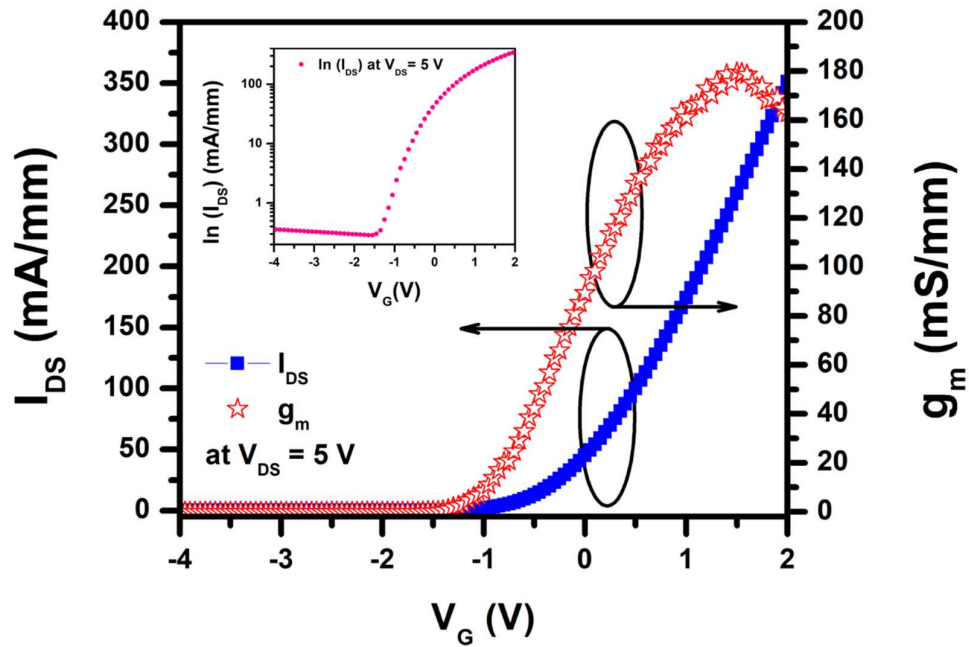
Table 4.1 shows the extracted parameters from the observed transfer characteristics of the HEMT device at  $300 \text{ K}$ , which is further used for simulation analysis. Here, the lower on-off ratio of the current is observed. It might be due to the un-passivated surface of the device, which may cause a higher leakage current.

**Table 4.1:** Extracted electrical parameters from the measured transfer characteristics of the HEMT device

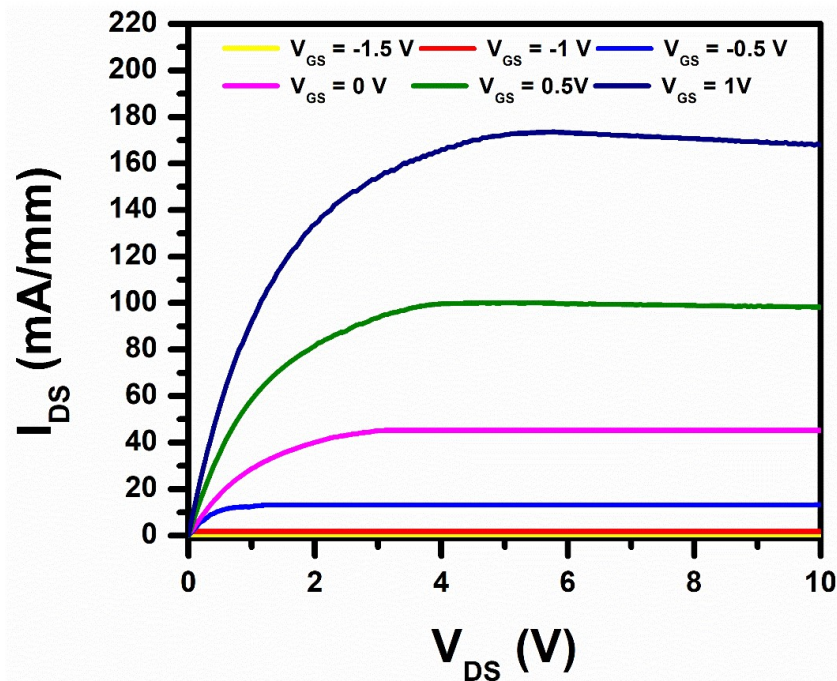
Extracted Electrical Parameters	Value
Peak transconductance ( $g_m$ )	$115 \pm 10 \text{ mS/mm}$
Threshold voltage ( $V_{th}$ )	$-0.56 \text{ V}$
$R_{on}$	$11.2 \Omega\text{-mm}$ at $V_{GS} = 2\text{V}$
$I_{ON}/I_{OFF}$	$2.32 \times 10^2$
mobility at 2DEG	$1270 \text{ cm}^2\text{V}^{-1}\text{s}^{-1}$

Figure 4.13 shows the  $I_D$ - $V_G$  and transconductance characteristics of the as-fabricated device for the sensing analysis at  $V_{DS} = 5\text{V}$ . The  $I_D$ - $V_G$  characteristic of the device on the logarithmic scale is depicted in the inset of Figure 4.13. Here, the threshold voltage ( $V_{th}$ ) and maximum transconductance ( $g_m$ ) of the device were observed as  $-0.38 \text{ V}$  and  $179 \text{ mS/mm}$ , respectively. Moreover,  $I_{ON}/I_{OFF}$  was observed as  $1.23 \times 10^3$ . It was observed here that the threshold voltage was shifted towards the positive side. It was due to the smaller thickness of the layers from the surface to the 2DEG channel (i.e., GaN cap layer, AlGaIn barrier layer, AlN spacer layer) compared to the previous device, which in turn increases the threshold voltage [Rabbaa and

Stiens, 2012]. The higher  $I_{ON}/I_{OFF}$  was due to  $\text{Si}_3\text{N}_4$  passivation of the device, which reduces the  $I_{OFF}$ . Furthermore, the  $I_{DS}V_{DS}$  characteristics of the device were also measured at different  $V_{GS}$  from -1.5 V to 1 V, and it is depicted in Figure 4.14. During the measurement, the  $I_{DS}$  is measured by varying  $V_{DS}$  from 0 V to 10 V at a particular  $V_{GS}$ . Moreover,  $R_{on}$  is also calculated as  $8.46 \Omega \cdot \text{mm}$  at  $V_{GS} = 1\text{V}$  by applying a similar process followed by Zhou *et al.* [Zhou *et al.*, 2017].



**Figure 4.13:** Drain current vs. Gate voltage ( $I_D$ - $V_G$ ) characteristics of the processed HEMT for sensing application at  $V_{DS}=5$  V along with the Transconductance ( $g_m$ ) curve. Logarithmic transfer characteristics of HEMT is shown in the inset.



**Figure 4.14:** Drain current vs. Drain voltage ( $I_D$ - $V_D$ ) characteristics of the as process AlGaIn/GaN HEMT for sensing application from  $V_{GS} = -1.5$  V to  $V_{GS} = 1$  V

## 4.5 CHAPTER CONCLUSION

In this chapter, the epitaxial growth and characterization of the AlGa<sub>N</sub>/Ga<sub>N</sub> HEMT were explained. Subsequently, the processes steps utilized for the fabrication of AlGa<sub>N</sub>/Ga<sub>N</sub> HEMT for the heavy metal ion sensing applications are also described in detail. These process steps contain the optimized parameters which helped in the successful fabrication of the AlGa<sub>N</sub>/Ga<sub>N</sub> HEMT sensor. Moreover, the contact resistance and sheet resistance were also calculated by the TLM method. In addition, transfer characteristics of the device also measured, and the calculation of electrical parameters like threshold voltage ( $V_{th}$ ), maximum transconductance ( $g_m$ ), on-resistance ( $R_{on}$ ) were also carried out. Hence, it can be said that the fabrication of AlGa<sub>N</sub>/Ga<sub>N</sub> HEMT using these process steps set a stage for the development of the heavy metal ion sensors. The development of these sensors using these fabricated devices will be explained in upcoming chapters.

...